

ChemComm

Accepted Manuscript



This is an *Accepted Manuscript*, which has been through the Royal Society of Chemistry peer review process and has been accepted for publication.

Accepted Manuscripts are published online shortly after acceptance, before technical editing, formatting and proof reading. Using this free service, authors can make their results available to the community, in citable form, before we publish the edited article. We will replace this *Accepted Manuscript* with the edited and formatted *Advance Article* as soon as it is available.

You can find more information about *Accepted Manuscripts* in the [Information for Authors](#).

Please note that technical editing may introduce minor changes to the text and/or graphics, which may alter content. The journal's standard [Terms & Conditions](#) and the [Ethical guidelines](#) still apply. In no event shall the Royal Society of Chemistry be held responsible for any errors or omissions in this *Accepted Manuscript* or any consequences arising from the use of any information it contains.

Cite this: DOI: 10.1039/c0xx00000x

www.rsc.org/xxxxxx

ARTICLE TYPE

Graphene-supported Pt and PtPd Nanorods with Enhanced Electrocatalytic Performance for Oxygen Reduction Reaction

Hong-Shuo Chen^a, Yu-Ting Liang^a, Tsan-Yao Chen^b, Yi-Chia Tseng^a, Chen-Wei Liu^c, Shu-Ru Chung^d, Chien-Te Hsieh^e, Cheng-En Lee^e, and Kuan-Wen Wang^{*a}

Received (in XXX, XXX) Xth XXXXXXXXX 20XX, Accepted Xth XXXXXXXXX 20XX

DOI: 10.1039/b000000x

The combinational modification of the morphology, alloying, and support for Pt catalyst has been optimized towards oxygen reduction reaction. Graphene-supported PtPd nanorods have lower unfilled Pt d-states than carbon-supported Pt nanoparticles (Pt/C) and their specific and mass activities after accelerated durability test is about 6.5 and 2.7 times higher than those of Pt/C, attributed to the synergistic electronic modification effect and graphene-metal interaction.

The development of highly effective and stable electrocatalysts toward oxygen reduction reaction (ORR) has attracted lots of attention recently.¹ Carbon-supported Pt nanomaterials with different alloying components and morphologies especially nanorods (NRs) or nanowires (NWs) have shown enhanced ORR performance when compared with Pt nanoparticles (NPs).² The ORR promotion for Pt or Pt-based 1-dimensional (1-D) nanomaterials may be related to their larger surface contact with the carbon support than the polyhedral NPs, better electron conductivity between the reaction sites and the carbon support, preferential exposure of certain crystal facets and less surface defects bearing.^{2e,3} Besides, recent studies have found that the electronic and chemical states of Pt NPs can be changed through the formation of 1-D structure and alloying effect, thus modifying the oxophilicity of Pt and enhancing the ORR performance.^{2b,2c}

Another approach for the optimization of the cathode catalysts is to use graphene as support. Because of high surface area, high conductivity, unique graphitized basal plane structure and potential low manufacturing cost, graphene has become a promising candidate as catalyst support in low-temperature fuel cells.⁴ It has been reported that the application of graphene as the support for Pt 1-D nanomaterials can successfully improve the dispersion and performance of the composite electrocatalyst materials and further improve the catalytic activity and stability by tuning the arrangement of surface active Pt atoms.⁵ However, this research paid little attention on the effect of alloying of graphene-supported Pt NRs on the ORR performance.⁵ Therefore, in this study, the graphene-supported Pt and PtPd NRs (G-Pt and G-PtPd) have been prepared and applied as electrocatalysts for ORR. Formic acid method was employed to prepare the 1-D nanomaterials without the use of sacrificial templates and surfactants. To the best of our knowledge, this is the first time that graphene has been used as supports for the Pt alloy NRs in

order to enhance ORR performance through electronic modification. The effect of morphological changes, Pd alloying and supports modifications on their ORR performance has been elucidated by the combination of the rotating disc electrode (RDE), high resolution transmission electron microscopy (HRTEM), and X-ray absorption spectroscopy (XAS) characterizations.

Figure 1 shows the morphologies changes of carbon-supported Pt NRs (C-Pt) and G-PtPd during accelerated durability test (ADT) characterized by HRTEM. In Figure 1 (a), NRs of C-Pt with a diameter of 3 nm and a length of 15 nm are grown on the surface of carbon supports while NRs with a larger diameter about 4.4 nm and a longer length about 25 nm can be obtained for G-Pt as displayed in Figure S1 in supporting information (SI). For G-PtPd NRs, their length is 35 nm as displayed in Figure 1 (b), suggesting that graphene can promote the anisotropic growth of Pt. Moreover, after ADT, it can be noted clearly that the rod-like structure almost disappears for C-Pt shown in Figure 1 (c) while NRs with different degrees of aggregations can still be observed for G-Pt, carbon-supported PtPd NRs (C-PtPd), or G-PtPd samples displayed in Figure S1 (c), Figure S1(d), or Figure 1(d), respectively, suggesting that either graphene support or Pd alloying may stabilize Pt during ADT, thus enhancing the ORR performance.

Figure S2 in SI shows the X-ray diffraction (XRD) patterns of various NRs. In the view point of bulk analysis, the C-PtPd and G-PtPd samples have fcc alloy structures. However, based on the extended X-ray absorption fine structure (EXAFS) results displayed in Figures S3 and S4, these alloys have a Pt rich in the inner core and Pd rich on the outer shell structure. Moreover, Table S1 shows the data analyses of XRD patterns. The peak areas integrated from (111), (200), and (220) planes for various NRs are calculated and used to describe the degrees of anisotropic growth,⁶ which influence the ORR performance significantly. It has been reported that the ORR performance increases on the order of Pt(100) << Pt(111) < Pt(110), in which the Pt(111) and Pt(110) planes have similar activity.^{1a} Therefore, the peak area ratio of [(111)+(220)]/(200) for Pt/C (46%, TKK) and various NRs are compared in Table S1. It seems that through alloying with Pd and using graphene support, the growth of (111) and (220) planes is promoted, suggesting that G-Pt and G-PtPd NRs have potentials to show better ORR performance due to the morphological effect.

Furthermore, Figure S5 displays the X-ray absorption near edge spectroscopy (XANES) spectrum at Pt L_{III} edge of Pt/C and various NRs. The absorption at 11564 eV is attributed to the 2p_{3/2}-5d electronic transitions and the magnitude of white line is related to the Pt oxidation state. As shown in Figure S5, the differences in the white lines indicate a change in Pt 5d band occupancy due to the adsorption of oxygenated species.⁷ The affinity of OH chemisorption on Pt depends on alloying.⁸ In this study, in order to investigate the effect of morphological changes of catalysts on the d-band vacancies of Pt, XANES results extracted from the Pt L_{III} and L_{II} white lines are applied to calculate the total number of unoccupied d-states, (H_{TS}).⁵ H_{TS} can be a good indicator to describe the effect of alloying, morphological changes, and modification on d-band of Pt.^{2b,2c,9} It has been reported that the d-band density of states (DOS) is structure-sensitive and the position of the d-band center shifts for different surfaces of Pt₃Ni single crystals,^{1b} thus affecting their ORR activity. However, for powder nanomaterials, the precise characterization of DOS under ultrahigh vacuum seems to be difficult and the calculation of H_{TS} becomes an alternative way to get an insight into the d-band. In this study, the H_{TS} value listed in Table S2 of Pt/C is decreased due to the formation of NRs, and further decreased due to the use of graphene support and alloying. In the viewpoint of d-band, the effect of using graphene as support and alloying with Pd for Pt is similar, whose H_{TS} is 0.307 and 0.306, respectively. Besides, the Pd alloying and graphene support can modify the d-band synergistically so that the H_{TS} of G-PtPd is as low as 0.295, suggesting that they have lower unfilled Pt d-states, and more d-band electrons transfer from Pd to Pt, which may lead to the enhanced ORR activity.^{2b,2c}

Figure 2 (a) shows the linear sweep voltammetry (LSV) results of Pt/C and various catalysts in O₂-saturated 0.5 M HClO₄ solution at 1600 rpm. The onset potentials of various catalysts follow the trend: G-PtPd > C-PtPd > G-Pt > C-Pt > Pt/C, which are inversely proportional to their H_{TS} values as compared in Table S2. Moreover, their kinetic current densities (I_k) also have the same sequence, suggesting that the modification of d-band can decisively promote their ORR performance. Besides, the specific activity (SA) and mass activity (MA), which is the I_k normalized to the electrochemical surface area (ECSA) and Pt loading are summarized in Table S2. The Pt loading is determined by inductively coupled plasma-atomic emission spectrometer and thermal gravimetric analysis, as displayed in Figure S6 in SI. The 1-D PtPd alloy NRs truly show their merits when compared with Pt/C and Pt NRs in which the SA and MA of G-PtPd is about 4.6 and 1.9 times higher than those of Pt/C, respectively. Furthermore, Figure 2 (b) compares their LSV results after 1000 cycles of ADT. During the potential cycling, the degradation of MA and SA occurs inevitably due to the dissolution, Ostwald ripening and aggregation of the metals and carbon corrosion.¹⁰ It can be seen that the slight changes in limiting current density after ADT may be due to the changes of catalyst dispersion and loading on the working electrode.¹¹ The I_k after ADT listed in Table S2 is in the order: G-PtPd > G-Pt > C-PtPd > C-Pt > Pt/C. It is worth mentioning that although C-PtPd has higher I_k before ADT than G-Pt, the latter one has better stability than the former one during ADT, suggesting that the graphene can provide excellent modification and stabilization

effect, probably because of the strong graphene-metal interaction.^{4a} Moreover, the MA retention, which is the ratios of MA/MA after ADT (MA₁₀₀₀) are compared in Table S2. It is noted that the NRs systems have much higher MA retention than Pt/C, confirming that 1-D nanomaterials are less vulnerable to dissolve in acidic media than 0-D materials. On the other hand, the MA retention of graphene-supported samples is higher than that of carbon-supported ones and Pt NRs have higher MA retention than PtPd NRs, demonstrating that graphene can provide more stable support to the metals and alloys.^{4a} The SA and MA of G-PtPd after ADT is about 6.5 and 2.7 times higher than those of Pt/C. It is interesting mentioning that although the graphene support and Pd alloying can both promote ORR of Pt NRs through the modification of H_{TS} , the stability of NRs can be specifically enhanced due to the graphene support. Moreover, Figure S7 summarizes the SA changes of Pt/C, C-Pt, and G-PtPd of ADT in O₂ and their SA after 2000 cycles is about 5, 40, and 81 $\mu\text{A}/\text{cm}^2$, respectively, confirming that graphene-supported PtPd NRs have superior ORR performance to carbon-supported Pt NPs and NRs during long-term test.

Figure 3 summarizes the correlation between H_{TS} and SA before and after ADT of Pt/C and various NRs. It can be seen that d-band of Pt/C can be modified by formation of NRs, and further decreased through using graphene support, addition of Pd, and the combination of the both. The SA of as-prepared catalysts basically follows the same trend in which lower H_{TS} suggests more d-band electrons transfer to Pt and higher ORR activity. Moreover, during the ADT, another factor, the resistance to the dissolution, corrosion and migration in acidic media, will influence the SA. The stabilization effect of graphene support is more significant than that from Pd alloying when the SA of G-Pt and C-PtPd is compared. This stabilization can be optimised by synergistic addition of graphene and Pd to Pt NRs. Among all, G-PtPd shows the superior ORR performance to Pt/C and other NRs, implying that the electronic modification effect from Pd and graphene-metal interaction can be promoted significantly for Pt.

The modification and stabilization effect from graphene and Pd also affect the surface chemical states of Pt, as shown in Figure S8 of the X-ray photoelectron spectroscopy (XPS) spectra. The fitting results suggest that the surface Pt/PtO ratios of Pt/C are changed due to the formation of NRs, using graphene support, and alloying with Pd. The formation of surface PtO is inhibited for the G-PtPd to 19 %, suggesting that the synergistic effect of Pd alloying and graphene support not only influence the electronic state of the bulk but also modify the surface chemical state of the NRs.

Conclusions

Graphene has been applied as supports to prepare Pt and PtPd NRs with enhanced ORR performance. The effect of graphene support and Pd alloying on the d-band vacancy and ORR performance has been elucidated. It is observed that G-PtPd has lower unfilled Pt d-states, and more d-band electrons transfer from Pd to Pt, and their SA and MA after ADT is about 6.5 and 2.7 times higher than those of Pt/C, confirming that the electronic modification effect from Pd and graphene-metal interaction can be promoted synergistically for Pt NRs.

Notes and references

^a Institute of Materials Science and Engineering, National Central University, Taoyuan 32001, Taiwan. E-mail: kuanwen.wang@gmail.com

^b Department of Engineering and System Science, National Tsing-Hua University, Hsinchu 30013, Taiwan

^c Green Energy and Environment Research Laboratories, Industrial Technology Research Institute, Hsinchu 310, Taiwan

^d Graduate Institute of Materials Science and Green Energy Engineering, National Formosa University, Yunlin 63201, Taiwan

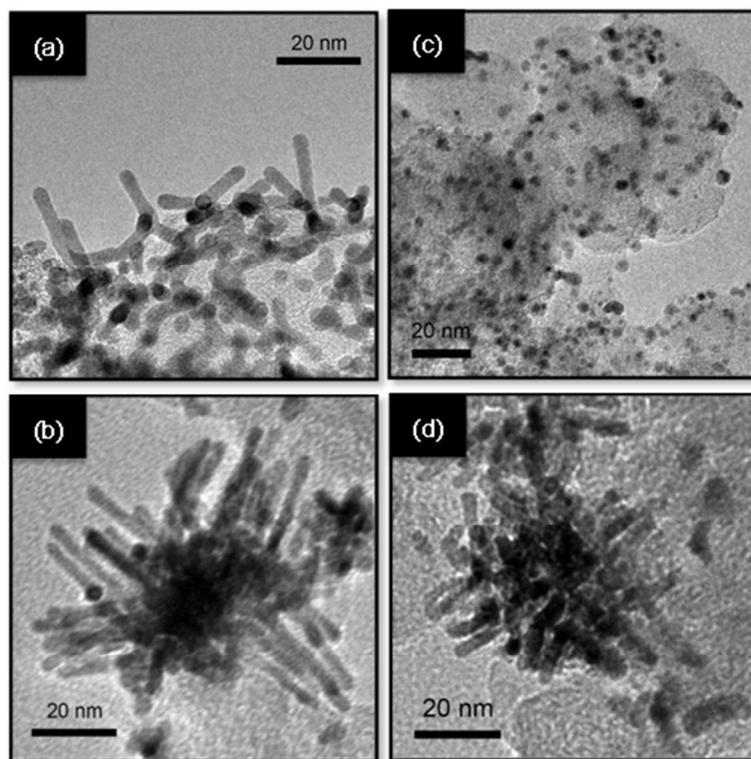
^e Department of Chemical Engineering and Materials Science, Yuan Ze University, Taoyuan 32003, Taiwan

† Electronic Supplementary Information (ESI) available: [XRD, EXAFS, XANES, TGA, ADT, and XPS]. See DOI: 10.1039/b000000x/

Acknowledgements

This work was supported by the National Science Council of Taiwan under Contract (no. 102-2221-E-008-030 and no. 102-2120-M-007-007).

1. a) B. Lim, M. Jiang, P.H.C. Camargo, E.C. Cho, J. Tao, X. Lu, Y. Zhu, Y. Xia, *Science* **2009**, *324*, 1302. b) V. R. Stamenkovic, B. Fowler, B. S. Mun, G. Wang, P. N. Ross, C. A. Lucas, N. M. Markovic, *Science* **2007**, *315*, 493. c) Y. S. Kim, S. H. Jeon, A. Bostwick, E. Rotenberg, P. N. Ross, V. R. Stamenkovic, N. M. Markovic, T. W. Noh, S. Han, B. S. Mun, *Adv. Energy Mater.* **2013**, *3*, 1257.
2. a) C. W. Liu, Y. C. Wei, C. C. Liu, K. W. Wang, *J. Mater. Chem.* **2012**, *22*, 4641. b) T. H. Yeh, C. W. Liu, H. S. Chen, K. W. Wang, *Electrochem. Commun.* **2013**, *31*, 125. c) Y. C. Tseng, H. S. Chen, C. W. Liu, T. H. Yeh, K. W. Wang, *J. Mater. Chem. A* **2014**, *2*, 4270. d) Y. Lu, Y. Jiang, W. Chen, *Nano Energy* **2013**, *2*, 836. e) S. Guo, S. Zhang, D. Su, S. Sun, *J. Am. Chem. Soc.* **2013**, *135*, 13879.
3. S. Sun, F. Jaouen and J. P. Dodelet, *Adv. Mater.* **2008**, *20*, 3900.
4. a) E. Antolini, *Appl. Catal. B Environ.* **2012**, *123-124*, 52-68. b) M. H. Seo, S. M. Choi, H. J. Kim, W. B. Kim, *Electrochem. Commun.* **2011**, *13*, 182.
5. R. Wang, D. C. Higgins, M. A. Hoque, D. U. Lee, F. Hassan, Z. Chen, *Sci. Rep.* **2013**, *3*, 2431.
6. C. T. Hsieh, J. M. Wei, H. T. Hsiao, W. Y. Chen, *Electrochim. Acta* **2012**, *64*, 177
7. S. Mukerjee, S. Srinivasan, M.P. Soriaga, *J. Phys. Chem.* **1995**, *99*, 4577.



70 Figure 1 HRTEM images for the as-prepared (a) C-Pt and (b) G-PtPd catalysts. (c) C-Pt and (d) G-PtPd catalysts after ADT.

8. E. Antolini, J.R.C. Salgado, M.J. Giz, E.R. Gonzalez, *Int. J. Hydrogen Energy* **2005**, *30*, 1213.
9. a) C. W. Liu, H. S. Chen, C. M. Lai, J. N. Lin, L. D. Tsai, K. W. Wang, *ACS Appl. Mater. Interfaces* **2014**, *6*, 1589. b) F. J. Lai, L. S. Sarma, H. L. Chou, D. G. Liu, C. A. Hsieh, J. F. Lee, B. J. Hwang, *J. Phys. Chem. C* **2009**, *113*, 12674.
10. X. Yu, S. Ye, *J. Power Sources* **2007**, *172*, 145.
11. a) Y. C. Wei, C. W. Liu, Y. W. Chang, C. M. Lai, P. Y. Lim, L. D. Tasi, K. W. Wang, *Int. J. Hydrogen Energy* **2010**, *35*, 1864. b) K. J. J. Mayrhofer, D. Strmcnik, B. B. Blizanac, V. Stamenkovic, M. Arenz, N. M. Markovic, *Electrochim. Acta*, **2008**, *53*, 3181.

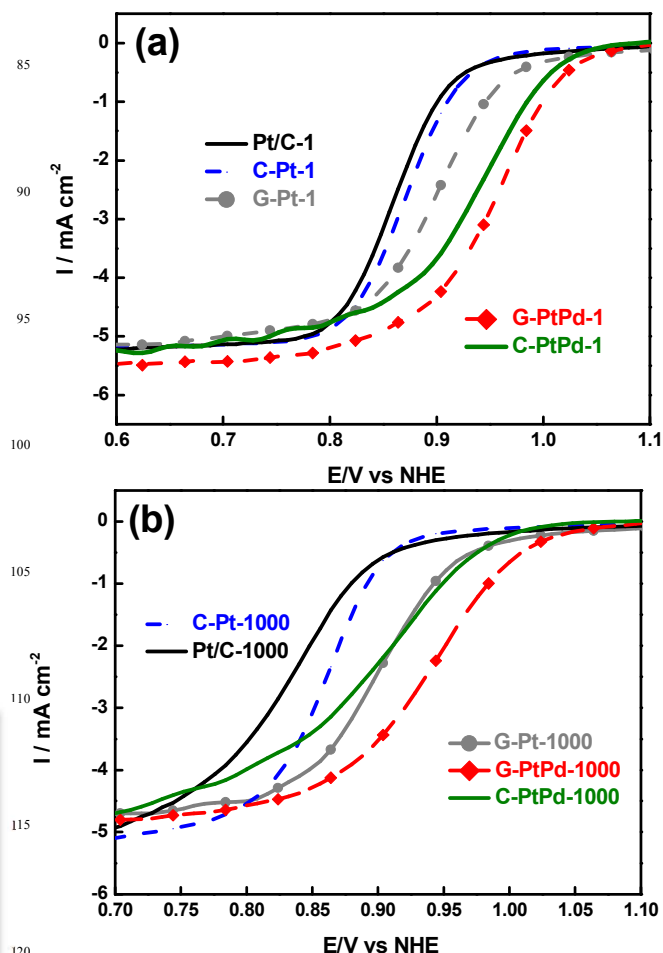


Figure 2 (a) LSV of Pt/C NP, C-Pt, C-PtPd, G-Pt, and G-PtPd NRs before and (b) after ADT.

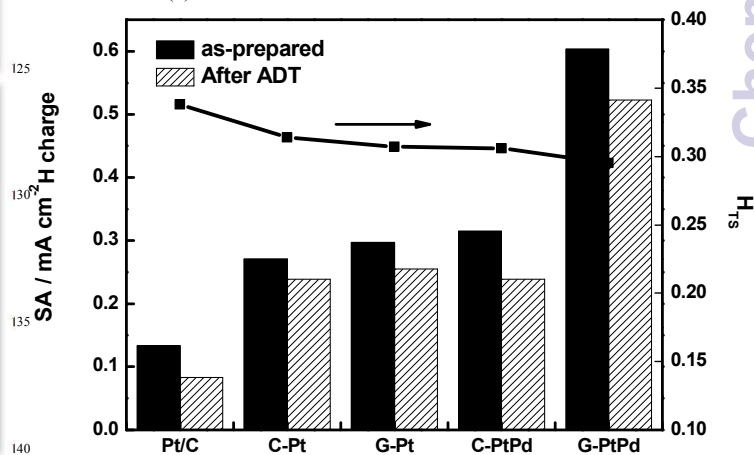


Figure 3 Comparison of SA and H_{TS} of the Pt/C NP, C-Pt, C-PtPd, G-Pt, and G-PtPd NR before and after ADT.